

# Critical Cavity-Magnon Polariton Mediated Strong Long-Distance Spin-Spin Coupling

Miao Tian,<sup>1</sup> Mingfeng Wang,<sup>1</sup> Guo-Qiang Zhang,<sup>2,\*</sup> Hai-Chao Li,<sup>3,†</sup> and Wei Xiong<sup>1,‡</sup>

<sup>1</sup>*Department of Physics, Wenzhou University, Zhejiang 325035, China*

<sup>2</sup>*School of Physics, Hangzhou Normal University, Hangzhou, Zhejiang 311121, China*

<sup>3</sup>*College of Physics and Electronic Science, Hubei Normal University, Huangshi 435002, China*

(Dated: April 28, 2023)

Strong long-distance spin-spin coupling is desperately demanded for solid-state quantum information processing, but it is still challenged. Here, we propose a hybrid quantum system, consisting of a coplanar waveguide (CPW) resonator weakly coupled to a single nitrogen-vacancy spin in diamond and a yttrium-iron-garnet (YIG) nanosphere holding Kerr magnons, to realize strong long-distance spin-spin coupling. With a strong driving field on magnons, the Kerr effect can squeeze magnons, and thus exponentially enhance the coupling between the CPW resonator and the squeezed magnons, which produces two cavity-magnon polaritons, i.e., the high-frequency polariton (HP) and low-frequency polariton (LP). When the enhanced cavity-magnon coupling approaches the critical value, the spin is fully decoupled from the HP, while the coupling between the spin and the LP is significantly improved. In the dispersive regime, a strong spin-spin coupling is achieved with accessible parameters, and the coupling distance can be up to  $\sim$ cm. Our proposal provides a promising way to manipulate remote solid spins and perform quantum information processing in weakly coupled hybrid systems.

## I. INTRODUCTION

Solid spins such as nitrogen-vacancy centers in diamond [1], having good tunability [2] and long coherence time [3–5], are regarded as promising platforms for quantum information science [14, 15]. However, direct spin-spin coupling is weak due to their small magnetic dipole moments [16–21]. Moreover, the coupling distance is directly determined by their separation. To overcome these, the natural ideal is to look for quantum interfaces [6–13] as bridges to couple long-distance spins, forming diverse hybrid quantum systems [14, 15].

Recently, the emerged low-loss magnons (i.e., the quanta of collective spin excitations) in ferromagnetic materials [22–25] have shown great potential in mediating distant spin-spin coupling [26–31]. For example, magnons in the Kittle mode of a nanometer-sized yttrium-iron-garnet (YIG) sphere have been used to strongly couple spins with tens of nanometers distance [26–28], via enhancing the local magnetic field. To further improve the coupling distance between two spins from nanometer to micronmeter, magnons with Kerr effect as quantum interface are proposed [32]. Also, the YIG nanosphere can be used to realize strong spin-photon coupling in a microwave cavity [33]. Besides these, magnons in a bulk material [29, 30] and thin ferromagnet film [31] have been suggested to coherently couple remote spins. However, achieved strong coupling is severely limited by the distance between two spins.

Motivated by this, we propose a hybrid spin-cavity-magnon system to realize a strong spin-spin coupling

with coupling distance  $\sim$  centimeter. In the proposed system, the spin in diamond is located at tens of nanometers from the central line of the CPW resonator, and weakly coupled to the CPW resonator. The nanometer-sized YIG sphere supporting Kerr magnons (i.e., magnons with Kerr effect) is employed but weakly coupled to the CPW resonator. Experimentally, strong and tunable magnon Kerr effect, originating from the magnetocrystalline anisotropy, has been demonstrated [34], giving rise to bi- and multi-stabilities [35–39], nonreciprocity [40], sensitive detection [41], quantum entanglement [42] and quantum phase transition [43, 44]. Under a strong driving field, this Kerr effect can squeeze magnons, and thus the coupling between magnons and the CPW resonator is exponentially enhanced to the strong coupling regime. The strong magnon-cavity coupling generates two polaritons, i.e., the high-frequency polariton (HP) and the low-frequency polariton (LP). When the enhanced magnon-cavity coupling strength approaches to the critical value, the LP becomes critical. Then the coupling between the spin and the HP is fully suppressed in the polariton representation, while the coupling between the spin and the LP is greatly enhanced. By further consider the case of two spins dispersively coupled to the LP, an indirect and strong spin-spin coupling can be induced by adiabatically eliminating the degrees of freedom of LP. Moreover, the coupling strength is not limited by the separation between two spins, it is actually determined by the length of the CPW resonator. Experimentally, the centimeter-sized CPW resonator has been fabricated [45]. Therefore, the achieved strong spin-spin coupling can be up to  $\sim$ cm. Our proposal provides an alternative path to remotely manipulate solid spin qubits and performing quantum information processing in weakly coupled spin-cavity-magnon systems.

\*zhangguoqiang@hznu.edu.cn

†hcl2007@foxmail.com

‡xiongweiphys@wzu.edu.cn

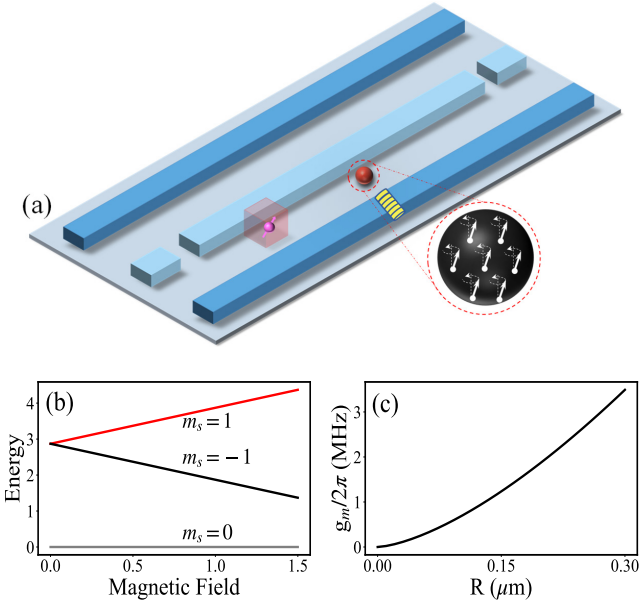


FIG. 1: (a) Schematic diagram of a hybrid quantum system. The single nitrogen vacancy (NV) center spin, located  $d$  distance away from the central line, is weakly coupled to the CPW resonator. The YIG sphere is driven by a microwave field through a microwave antenna. (b) The level structure of the triplet ground state of the NV center,  $m_s = 0$  and  $m_s = -1$  are selected to form a spin qubit. (c) The cavity-magnon coupling versus the radius  $R$  of the YIG nanosphere.

## II. MODEL AND HAMILTONIAN

We consider a hybrid quantum system consisting of a coplanar waveguide (CPW) resonator weakly coupled to both a single NV spin in diamond and a nanometer-sized YIG sphere, as shown in Fig. 1(a). The spin is fabricated far away from the YIG sphere to avoid their direct coupling. In addition, the magnon Kerr effect, stemming from the magnetocrystallographic anisotropy [35, 36], is taken into account. Thus, the total Hamiltonian of the hybrid system can be written as (setting  $\hbar = 1$ ),

$$H_{\text{tot}} = H_{\text{NV}} + H_{\text{CM}} + H_{\text{CS}} + H_K + H_D, \quad (1)$$

where  $H_{\text{NV}} = \frac{1}{2}\omega_{\text{NV}}\sigma_z$ , with the transition frequency  $\omega_{\text{NV}} = D - g_e\mu_B B_{ex}$  between the lowest two levels of the triplet ground state of the NV [see Fig. 1(b)], is the free Hamiltonian of the NV spin. Here,  $D = 2\pi \times 2.87$  GHz is the zero-field splitting,  $g_e = 2$  is the Landé factor,  $\mu_B$  is the Bohr magneton, and  $B_{ex}$  is the external magnetic field to lift the near-degenerate states  $|m_s = \pm 1\rangle$ . The second term

$$H_{\text{CM}} = \omega_c a^\dagger a + g_m (a^\dagger m + a m^\dagger) \quad (2)$$

represents the Hamiltonian of the coupled magnon-cavity subsystem, where  $\omega_c$  is the frequency of the CPW resonator and  $g_m$  is the coupling strength [33], nearly proportional to the radius  $R$  of the YIG sphere [see Fig. 1(c)].

Obviously, strong coupling can be obtained by using micronmeter-sized sphere, which is widely employed in experiments [46–49]. For the nanometer-sized sphere such as  $R \sim 50$  nm, we have  $g_m \sim 2\pi \times 0.2$  MHz, which is much smaller than the typical decay rates of the cavity ( $\kappa_c/2\pi \sim 1$  MHz) [50] and Kittle mode ( $\kappa_m/2\pi \sim 1$  MHz) [51], i.e.,  $g_m < \kappa_c, \kappa_m$ . This indicates that the coupling between the Kittle mode of the nanosphere and the cavity is in the weak coupling regime, consistent with our assumption.

The Hamiltonian  $H_{\text{CS}}$  in Eq. (1) describes the interaction between the spin qubit and the cavity. With the rotating-wave approximation,  $H_{\text{CS}}$  can be governed by [19, 20]

$$H_{\text{CS}} = \lambda (\sigma_+ a + a^\dagger \sigma_-), \quad (3)$$

where  $\lambda = 2g_e\mu_B B_{0,\text{rms}}(d)$  [19] is the coupling strength, with  $B_{0,\text{rms}}(d) = \mu_0 I_{\text{rms}}/2\pi d$ ,  $I_{\text{rms}} = \sqrt{\hbar\omega_c/2L_a}$ , and  $d$  being the distance between the spin and the center conductor of the CPW resonator. To estimate  $\lambda$ ,  $\omega_c \sim 2\pi \times 2$  GHz and  $L_a \sim 2$  nH [51] are chosen. For  $d \sim 5$   $\mu\text{m}$ ,  $\lambda \sim 2\pi \times 70$  Hz, and  $d \sim 50$  nm,  $\lambda \sim 2\pi \times 7$  kHz [19], leading to  $\lambda < \kappa_c$ . This shows that the coupling between the spin qubit and the cavity is also in the weak coupling regime. Due to this fact, we here assume that the spin qubit is placed close to the central line of the CPW resonator to obtain a moderate coupling strength, although it is still weakly coupled to the cavity. Experimentally, such weak spin-cavity weak couplings can be measured.

The Hamiltonian  $H_K$  in Eq. (1) denotes the magnon Kerr effect, characterizing the coupling among magnons in the YIG sphere and provides the anharmonicity of the magnons, which is given by [36]

$$H_K = \omega_m m^\dagger m + K m^\dagger m^\dagger m m, \quad (4)$$

where  $\omega_m = \gamma B_0 - 2\mu_0 K_{\text{an}} \gamma^2 s/M^2 V_m + \mu_0 K_{\text{an}} \gamma^2/M^2 V_m$  is the frequency of the Kittle mode, with the gyromagnetic ratio  $\gamma/2\pi = g_e\mu_B/\hbar$  ( $\mu_B$  is the Bohr magneton), the vacuum permeability  $\mu_0$ , the first-order anisotropy constant of the YIG sphere  $K_{\text{an}}$ , the amplitude of a bias magnetic field  $B_0$ , the saturation magnetization  $M$ , and the volume of the YIG sphere  $V_m$ .  $K = \mu_0 K_{\text{an}} \gamma^2/M^2 V_m$  is the coefficient. Apparently, the Kerr coefficient is inversely proportional to the volume of the YIG sphere, i.e.,  $K \propto 1/V_m$ , the Kerr effect can become significantly important for a YIG nanosphere. For example, when  $R \sim 50$  nm,  $K/2\pi \sim 128$  Hz, but  $K/2\pi \sim 0.05$  nHz for  $R \sim 0.5$  mm (the usual size of the YIG sphere used in various previous experiments). Obviously,  $K$  is much smaller in the latter case. Because our proposal mainly relies on the Kerr effect, we here use the nanometer-sized YIG sphere to obtain strong Kerr effect. The last term

$$H_D = \Omega_d (m^\dagger e^{-i\omega_d t} + m e^{i\omega_d t}). \quad (5)$$

in Eq. (1) describes the interaction between the Kittle mode and the driving field, where  $\Omega_d$  is the Rabi frequency and  $\omega_d$  is the frequency of the driving field.

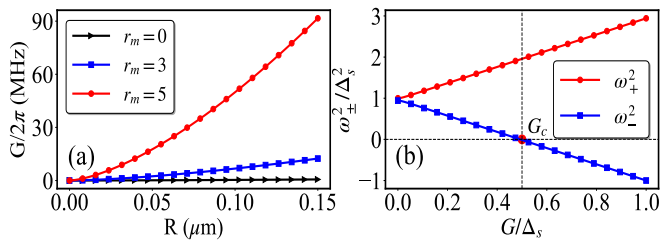


FIG. 2: (a) The coupling strength between the squeezed magnons and the CPW resonator versus the radius of the YIG nanosphere with different squeezing parameters  $r_m = 0, 3, 5$ . (b) The square of polariton frequencies versus the coupling between the squeezed magnons and the CPW resonator.

In the rotating frame with respect to the driving frequency ( $\omega_d$ ), the total Hamiltonian in Eq. (1) becomes

$$H_{\text{sys}} = \frac{1}{2}\Delta_{\text{NV}}\sigma_z + \Delta_c a^\dagger a + H'_K + \Omega_d(m^\dagger + m) + \lambda(\sigma_+ a + a^\dagger \sigma_-) + g_m(a^\dagger m + am^\dagger), \quad (6)$$

where  $\Delta_{\text{NV}} = \omega_{\text{NV}} - \omega_d$  is the frequency detuning of the spin qubit from the driving field,  $\Delta_c = \omega_c - \omega_d$  is the frequency detuning of the cavity field from the driving field, and  $H'_K = \delta_m m^\dagger m + K m^\dagger m^\dagger m m$  [32], with  $\delta_m = \omega_m - \omega_d$  being the frequency detuning of the Kittle mode from the driving field. Due to the large  $\Omega_d$ , the Hamiltonian  $H_{\text{sys}}$  in Eq. (6) can be linearized by writing each system operator as the expectation value plus its fluctuation [52]. By neglecting the higher-order fluctuation terms, Eq. (6) is linearize as

$$H_{\text{lin}} = \frac{1}{2}\Delta_{\text{NV}}\sigma_z + \Delta_c a^\dagger a + \mathcal{H}_K + \lambda(\sigma_+ a + a^\dagger \sigma_-) + g_m(a^\dagger m + am^\dagger), \quad (7)$$

with

$$\mathcal{H}_K = \Delta_m m^\dagger m + K_s(m^2 + m^{\dagger 2}), \quad (8)$$

where the effective magnon frequency detuning  $\Delta_m = \delta_m + 4K|\langle m \rangle|^2$  is induced by the Kerr effect, which has been demonstrated experimentally [35, 36]. The amplified coefficient  $K_s = K|\langle m \rangle|^2$  is the effective strength of the two-magnon process, which can give rise to squeeze magnons in the Kittle mode. Aligning the biased magnetic field along the crystalline axis [100] or [110] of the YIG sphere [34, 36],  $K$  can be positive or negative, and we can have  $K_s > 0$  or  $K_s < 0$ . There we choose  $K_s < 0$  when  $K < 0$ . The linearized Kerr Hamiltonian  $\mathcal{H}_K$  in Eq. (8) describes the two-magnon process, which can give rise to the magnon squeezing.

Below we operate the proposed hybrid system in the magnon-squeezing frame by diagonalizing the Hamiltonian  $\mathcal{H}_K$  with the Bogoliubov transformation  $m = m_s \cosh(r_m) + m_s^\dagger \sinh(r_m)$ , where  $r_m = \frac{1}{4} \ln \frac{\Delta_m - 2K_s}{\Delta_m + 2K_s}$  is the squeezing parameter. After diagonalization,  $\mathcal{H}_K$  becomes

$$\mathcal{H}_{\text{KS}} = \Delta_s m_s^\dagger m_s \quad (9)$$

with  $\Delta_s = \sqrt{\Delta_m^2 - 4K_s^2}$  being the frequency of the squeeze magnon, and Eq. (7) is transformed to

$$H_S = \frac{1}{2}\Delta_{\text{NV}}\sigma_z + H_{\text{CMS}} + \lambda(\sigma_+ a + a^\dagger \sigma_-), \quad (10)$$

where

$$H_{\text{CMS}} = \Delta_c a^\dagger a + \Delta_s m_s^\dagger m_s + G(a^\dagger + a)(m_s^\dagger + m_s) \quad (11)$$

is the effective Hamiltonian of the CPW resonator coupled to the squeezed magnons,  $G = \frac{1}{2}g_m e^{r_m}$  is the exponentially enhanced coupling strength between the squeezed magnons and the CPW resonator. Because both the parameters  $\Delta_m$  and  $K_s$  can be tuned, so  $r_m$  can be very large when  $\Delta_m \sim -2K_s$ , leading to the strong  $G$  even for nanometer-sized YIG sphere [see curves in Fig. 2(a)]. Specifically, when  $r_m = 0$ , i.e., magnons in the Kittle mode is not squeezed, the coupling strength between the CPW resonator and the Kittle mode is unamplified, giving rise to weak  $G$  [see the black curve in Fig. 2(a)]. When magnons in the Kittle mode are squeezed but with moderate squeezing parameters such as  $r_m = 3$  and  $r_m = 5$ , we find the coupling strength  $G$  can be significantly improved for the YIG nanosphere. For example,  $R \sim 50$  nm and  $r_m \sim 3$ , we have  $G/2\pi = 2$  MHz, which is comparable with the decay rates of the CPW resonator ( $\kappa_c$ ) and the Kittle mode ( $\kappa_m$ ). But when  $r_m \sim 5$ ,  $G/2\pi = 17$  MHz, which is much larger than both  $\kappa_c$  and  $\kappa_m$ . These indicates that indicates that strong coupling between the squeezed magnons and the CPW resonator can be realized by tuning the squeezing parameter  $r_m$ . In addition,  $G$  can be further enhanced by using the larger radius of the YIG sphere when  $r_m$  is fixed. Once the strong coupling between the squeezed magnons and the CPW resonator is achieved, the counterrotating terms  $\propto a^\dagger m_s^\dagger$  and  $am_s$  in Eq. (11) are related to two-mode squeezing, while rotating terms  $\propto a^\dagger m_s$  and  $am_s^\dagger$  allow quantum state transfer between the squeezed magnons and the CPW resonator. By combining these, polaritons with criticality can be formed, as shown below.

### III. STRONG COUPLING BETWEEN THE SINGLE NV SPIN AND THE LOW-FREQUENCY POLARITON

By further diagonalizing the Hamiltonian  $H_{\text{CMS}}$  in Eq. (11), two polaritons with eigenfrequencies

$$\omega_{\pm}^2 = \frac{1}{2} \left[ \Delta_c^2 + \Delta_s^2 \pm \sqrt{(\Delta_c^2 - \Delta_s^2)^2 + 16G^2\Delta_c\Delta_s} \right] \quad (12)$$

can be obtained. This is owing to the fact of the achieved strong coupling between the squeezed magnons and the CPW resonator. For convenience, we call two polaritons with frequencies  $\omega_+$  and  $\omega_-$  as the high- and low-frequency polaritons (HP and LP). The diagonalized  $H_{\text{CMS}}$  reads

$$H_{\text{diag}} = \omega_+ a_+^\dagger a_+ + \omega_- a_-^\dagger a_-, \quad (13)$$

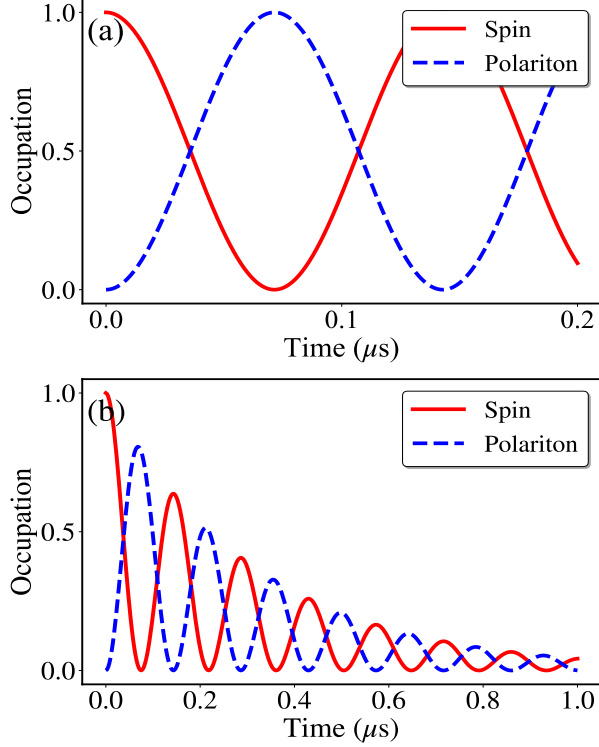


FIG. 3: The occupation of the LP and spin qubit versus the evolution time at  $G \rightarrow G_c$  and  $\Delta_c \gg \Delta_s$  (a) without and (b) with dissipations. The spin decay rate is  $\gamma_{\perp} \sim 1$  kHz and the LP decay rate is  $\kappa_{-} \sim 1$  MHz. In both (a) and (b), the spin qubit is initially prepared in the excited state and the LP is in the ground state, and the coupling strength is  $g_r/2\pi \sim 3.5$  MHz.

where

$$a = \frac{\cos \theta}{2\sqrt{\Delta_c \omega_{-}}} \left[ a_{-} (\Delta_c + \omega_{-}) + a_{-}^{\dagger} (\Delta_c - \omega_{-}) \right] + \frac{\sin \theta}{2\sqrt{\Delta_c \omega_{+}}} \left[ a_{+} (\Delta_c + \omega_{+}) + a_{+}^{\dagger} (\Delta_c - \omega_{+}) \right]. \quad (14)$$

Substituting Eqs. (13) and (14) into Eq. (10), the Hamiltonian of the coupled spin-CMP can be given by

$$H_{\text{CMP}} = \frac{1}{2} \Delta_{\text{NV}} \sigma_z + \omega_{+} a_{+}^{\dagger} a_{+} + \omega_{-} a_{-}^{\dagger} a_{-} + g_r (\sigma_{+} a_{-} + \sigma_{-} a_{+}^{\dagger}) + g_{\text{cr}} (\sigma_{+} a_{-}^{\dagger} + \sigma_{-} a_{+}) + g'_r (\sigma_{+} a_{+} + \sigma_{-} a_{+}^{\dagger}) + g'_{\text{cr}} (\sigma_{+} a_{+}^{\dagger} + \sigma_{-} a_{+}), \quad (15)$$

where  $g_{c(\text{cr})} = \lambda \cos \theta (\Delta_c \pm \omega_{-}) / 2\sqrt{\Delta_c \omega_{-}}$  denote the effective coupling strength between the NV spin and the LP,  $g'_{c(\text{cr})} = \lambda \sin \theta (\Delta_c \pm \omega_{+}) / 2\sqrt{\Delta_c \omega_{+}}$  represent the effective coupling strength between the NV spin and the HP. Obviously, both  $g_{c(\text{cr})}$  and  $g'_{c(\text{cr})}$  can be *tuned* by the driving field on the Kittle mode of the YIG sphere. The parameter  $\theta$  is defined by  $\tan(2\theta) = 4G\sqrt{\Delta_c \Delta_s} / (\Delta_c^2 - \Delta_s^2)$ . To show the behavior of two polaritons with the

coupling strength  $G$ , we plot the square of polariton frequencies versus the coupling strength  $G$  in Fig. 2(b). Clearly, one can see that  $\omega_{+}^2$  increases with  $G$ , but  $\omega_{-}^2$  decreases. When  $\omega_{-}^2 = 0$ ,  $G$  reduces to the critical coupling strength  $G_c$ , i.e.,

$$G = G_c \equiv \frac{1}{2} \sqrt{\Delta_c \Delta_s}, \quad (16)$$

which means  $\omega_{-}$  is real for  $G < G_c$ , while  $\omega_{-}$  is imaginary (the low-polariton is unstable) for  $G > G_c$ . When we operate the coupled cavity-magnon subsystem around the critical point (i.e.,  $G \rightarrow G_c$ ) and  $\Delta_c \gg \Delta_s$  is satisfied, we have  $g_r \approx g_{\text{cr}} \rightarrow \frac{1}{2} \lambda \sqrt{\Delta_c / \omega_{-}}$ ,  $g'_r \approx g'_{\text{cr}} \rightarrow 0$ . Due to the large  $\Delta_c$  and the extremely small  $\omega_{-}$ ,  $g_r \approx g_{\text{cr}} \gg \lambda$ . These indicate that coupling between the NV spin and the HP is completely decoupled, while the coupling between the NV spin and the LP is significantly enhanced. By choosing  $\Delta_c = 10^6 \omega_{-}$ ,  $g_r = g_{\text{cr}} \sim 10^3 \lambda$  are estimated. Obviously, three orders of magnitude of the spin-low-polariton coupling is improved. Using  $d = 50$  nm,  $\lambda = 2\pi \times 7$  kHz is obtained, resulting in  $g_r/2\pi = 3.5$  MHz, which is larger than the decay rates of the CPW resonator and the Kittle mode, i.e.,  $g_{r(\text{cr})} > \kappa_c, \kappa_m$ . This suggests that the coupling between the spin and the LP can be in the strong coupling regime. In principle,  $g_{r(\text{cr})}$  can be further enhanced by using the larger  $\Delta_c$  or much smaller  $\omega_{-}$ . In the strong coupling regime, the rotating-wave approximation is still valid, and the counterrotating term related to  $g_{\text{cr}}$  in Eq. (15) can be safely ignored, so Eq. (15) reduces to

$$H_{\text{JC}} = \frac{1}{2} \Delta_{\text{NV}} \sigma_z + \omega_{-} a_{-}^{\dagger} a_{-} + g_r (\sigma_{+} a_{-} + \sigma_{-} a_{-}^{\dagger}), \quad (17)$$

which is the so-called Janes-Cumming model with the strong coupling, allowing quantum state exchange between the spin and the LP, as demonstrated in Fig. 3(a), where the spin is initially prepared in the excited state and the the LP is in the ground state.

When dissipations are included, the dynamics of the system can be described by the master equation,

$$\frac{d\rho}{dt} = -i [H_{\text{JC}}, \rho] + \kappa_{-} \mathcal{D}[a_{-}] \rho + \gamma_{\perp} \mathcal{D}[\sigma_{-}] \rho, \quad (18)$$

where  $\mathcal{D}[o]\rho = o\rho o^{\dagger} - \frac{1}{2}(o^{\dagger}o\rho + \rho o^{\dagger}o)$ , and  $\gamma_{\perp}$  is the transversal relaxation rate of the NV spin [53],  $\kappa_{-}$  is the decay rate of the LP. In Fig. 3(b), we use the qutip package in python [54, 55] to numerically simulate the dynamics of the spin and LP governed by Eq. (18). The results show that state exchange between the spin and the LP can be realized in the presence of dissipations such as  $\kappa_{-} \sim 1$  MHz and  $\gamma_{\perp} \sim 1$  kHz [58], although the occupation probability decreases with long evolution time.

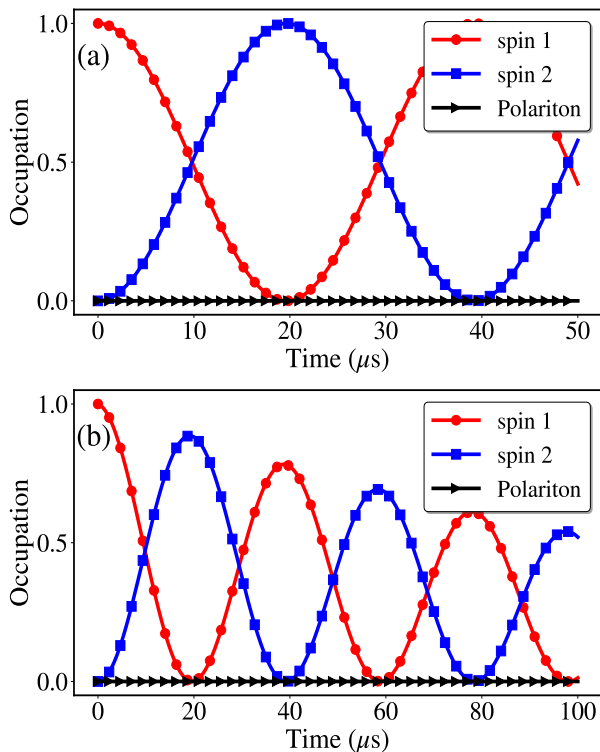


FIG. 4: The occupation of two spins and the LP versus the evolution time in the dispersive regime (a) without and (b) with dissipations. The parameters are the same as in Fig. 3.

#### IV. THE EFFECTIVE STRONG COUPLING BETWEEN TWO SINGLE NV SPINS

Here, we further consider the case that two identical NV spins are symmetrically placed away from the YIG sphere in the CPW resonator. Thus, two spins interact with the CPW resonator with the same coupling strength  $\lambda$ . By operating the cavity-magnon subsystem around the critical point, the couplings between two spins and the HP can be fully suppressed, while the couplings between two spins and the LP is greatly enhanced, similar to the single spin case. Therefore, the Hamiltonian of the hybrid system with two identical spins can be effectively described by Tavis-Cummings model,

$$H_{TC} = \omega_- a_-^\dagger a_- + \frac{1}{2} \Delta_{NV} (\sigma_z^{(1)} + \sigma_z^{(2)}) + g_r \left[ (\sigma_+^{(1)} + \sigma_+^{(2)}) a_- + \text{h.c.} \right]. \quad (19)$$

In the dispersive regime, i.e.,  $|\Delta_{NV} - \omega_-| \gg g_r$ , the LP can be as an interface to induce an indirect coupling between two spins by using the Fröhlich-Nakajima transformation [56, 57]. By adiabatically eliminating the degrees of freedom of the LP, we can obtain the effective spin-spin Hamiltonian as

$$H_{\text{eff}} = \frac{1}{2} \omega_{\text{eff}} (\sigma_z^{(1)} + \sigma_z^{(2)}) + g_{\text{eff}} (\sigma_+^{(1)} \sigma_-^{(2)} + \sigma_-^{(1)} \sigma_+^{(2)}), \quad (20)$$

where  $\omega_{\text{eff}} = \Delta_{NV} + 2g_{\text{eff}} n_- + g_{\text{eff}}$  is the effective transition frequency of the NV spin, depending on the mean occupation number  $n_- = \langle a_-^\dagger a_- \rangle$  of the LP,  $g_{\text{eff}} = -g_r^2 / \Delta_{NV}$  is the effective spin-spin coupling strength induced by the LP. To estimate  $g_{\text{eff}}$ , we assume the distance between the spin and the central line of the CPW resonator  $d = 50$  nm, so  $g_r / 2\pi = 3.5$  MHz, thus we have  $g_{\text{eff}} / 2\pi = 12.7$  kHz when  $\Delta_{NV} / 2\pi = 960$  MHz. Obviously,  $g_{\text{eff}} \gg \gamma_\perp \sim 1$  kHz, i.e., the strong spin-spin coupling is achieved. This can be directly demonstrated by simulating the dynamics of the effective system, governed by Eq. (20) or Eq. (19) in the dispersive regime, with the master equation. The simulating results are presented in Fig. 4. One can see that quantum states of two spins can be exchanged each other with [see Fig. 4(a)] and without [see Fig. 4(b)] dissipations, while the LP is always in the initial state. Note that the achieved strong spin-spin coupling is not limited by the separation between two spins, it is only determined by the length of the CPW resonator. Experimentally, the centimeter-sized cavity has been fabricated, so the distance of the strong spin-spin coupling can be improved to centimeter level. Compared to previous proposals of directly coupled spins to a YIG nanosphere [26–28], the distance here is nearly enhanced by *six* orders of magnitude.

#### V. CONCLUSIONS

In summary, we have proposed a hybrid system consisting of a CPW resonator weakly coupled to NV spins and a YIG nanosphere supporting magnons with Kerr effect. With the strong driving field, the Kerr effect can squeeze magnons, giving rise to exponentially enhanced strong cavity-magnon coupling, and thus CMPs can be formed. By approaching the cavity-magnon coupling strength to the critical value, the spin-LP coupling is greatly enhanced to the strong coupling regime with the accessible parameters, while the coupling between the spins and the HP is fully suppressed. Using the LP as quantum interface in the dispersive regime, strong long-distance spin-spin coupling can be achieved, which allows quantum state exchange between two spins. With current fabricated technology of the CPW resonator, the distance of the strong spin-spin coupling can be up to  $\sim$ cm level, which is improved about six orders of magnitude than the previous proposal of directly coupled spins to a YIG nanosphere. Our scheme provides a potential path to realize a long-distance strong spin-spin coupling with critical CMPs in weakly coupled hybrid systems.

This paper is supported by the National Natural Science Foundation of China (Grants No. 12205069, No. 11904201 and No. 11804074).

- [1] R. Schirhagl, K. Chang, M. Loretz, and C. L. Degen, Nitrogen-Vacancy Centers in Diamond: Nanoscale Sensors for Physics and Biology, *Annu. Rev. Phys. Chem.* **65**, 83 (2014).
- [2] M. W. Doherty, N. B. Manson, P. Delaney, F. Jelezko, J. Wrachtrupe, L. C. L. Hollenberg, The nitrogen-vacancy colour centre in diamond, *Phys. Rep.* **528**, 1 (2013).
- [3] N. Bar-Gill, L. Pham, A. Jarmola, D. Budker, and R. Walsworth, Solid-state electronic spin coherence time approaching one second, *Nat. Commun.* **4**, 1743 (2013).
- [4] F. Jelezko, T. Gaebel, I. Popa, A. Gruber, and J. Wrachtrup, Observation of Coherent Oscillations in A Single Electron Spin, *Phys. Rev. Lett.* **92**, 076401 (2004).
- [5] G. Balasubramian, P. Neumann, D. Twitchen, M. Markham, R. Koselov, N. Mizuochi, J. Isoya, J. Achard, J. Beck, J. Tissler, V. Jacques, P. R. Hemmer, F. Jelezko, and J. Wrachtrup, Ultralong spin coherence time in isotopically engineered diamond, *Nat. Mater.* **8**, 383 (2009).
- [6] P. B. Li, Z. L. Xiang, P. Rabl, and F. Nori, Hybrid Quantum Device with Nitrogen-Vacancy Centers in Diamond Coupled to Carbon Nanotubes, *Phys. Rev. Lett.* **117**, 015502 (2016).
- [7] P. Rabl, S. J. Kolkowitz, F. H. L. Koppens, J. G. E. Harris, P. Zoller, and M. D. Lukin, A quantum spin transducer based on nanoelectromechanical resonator arrays, *Nat. Phys.* **6**, 602 (2010).
- [8] L. Tian, Robust Photon Entanglement via Quantum Interference in Optomechanical Interfaces, *Phys. Rev. Lett.* **110**, 233602 (2013).
- [9] J. Chen, Z. Li, X. Q. Luo, W. Xiong, M. Wang, H. C. Li, Strong single-photon optomechanical coupling in a hybrid quantum system, *Opt. Express* **29**, 32639 (2021).
- [10] M. Aspelmeyer, T. J. Kippenberg, and F. Marquardt, Cavity optomechanics, *Rev. Mod. Phys.* **86**, 1391 (2014).
- [11] W. Xiong, M. Wang, G. Q. Zhang, and J. Chen, Optomechanical-interface-induced strong spin-magnon coupling, *Phys. Rev. A* **107**, 033516 (2023).
- [12] W. Xiong, Z. Li, Y. Song, J. Chen, G. Q. Zhang, and M. Wang, Higher-order exceptional point in a pseudo-Hermitian cavity optomechanical system, *Phys. Rev. A* **104**, 063508 (2021).
- [13] W. Xiong, Z. Li, G. Q. Zhang, M. Wang, H. C. Li, X. Q. Luo, and J. Chen, Higher-order exceptional point in a blue-detuned non-Hermitian cavity optomechanical system, *Physical Review A* **106**, 033518 (2022).
- [14] Z. L. Xiang, S. Ashhab, J. Q. You, and F. Nori, Hybrid quantum circuits: Superconducting circuits interacting with other quantum systems, *Rev. Mod. Phys.* **85**, 623 (2013).
- [15] G. Kurizki, P. Bertet, Y. Kubo, K. Mølmer, D. Petrosyan, P. Rabl, and J. Schmiedmayer, Quantum technologies with hybrid systems, *Proc. Natl. Acad. Sci. USA* **112**, 3866 (2015).
- [16] Y. Kubo, F. R. Ong, P. Bertet, D. Vion, V. Jacques, D. Zheng, A. Dréau, J.-F. Roch, A. Auffeves, F. Jelezko, J. Wrachtrup, M. F. Barthe, P. Bergonzo, and D. Esteve, Strong Coupling of A Spin Ensemble to A Superconducting Resonator, *Phys. Rev. Lett.* **105**, 140502 (2010).
- [17] D. Marcos, M. Wubs, J. M. Taylor, R. Aguado, M. D. Lukin, and A. S. Sørensen, Coupling Nitrogen-Vacancy Centers in Diamond to Superconducting Flux Qubits, *Phys. Rev. Lett.* **105**, 210501 (2010).
- [18] X. Zhu, S. Saito, A. Kemp, K. Kakuyanagi, S. Karimoto, H. Nakano, W. J. Munro, Y. Tokura, M. S. Everitt, K. Nemoto, M. Kasu, N. Mizuochi, and K. Semba, Coherent coupling of a superconducting flux qubit to an electron spin ensemble in diamond, *Nature (London)* **478**, 221 (2011).
- [19] J. Twamley and S. D. Barrett, Superconducting cavity bus for single nitrogen-vacancy defect centers in diamond, *Phys. Rev. B* **81**, 241202(R) (2010).
- [20] W. Xiong, J. Chen, B. Fang, M. Wang, L. Ye, and J. Q. You, Strong tunable spin-spin interaction in a weakly coupled nitrogen vacancy spin-cavity electromechanical system, *Phys. Rev. B* **103**, 174106 (2021).
- [21] W. Xiong, J. Chen, B. Fang, C. H. Lam, and J. Q. You, Coherent perfect absorption in a weakly coupled atom-cavity system, *Phys. Rev. A* **101**, 063822 (2020).
- [22] B. Z. Rameshti, S. V. Kusminskiy, J. A. Haigh, K. Usami, D. Lachance-Quirion, Y. Nakamura, C. M. Hu, H. X. Tang, G. E. W. Bauer, and Y. M. Blanter, Cavity magnonics, *Phys. Rep.* **979**, 1 (2022).
- [23] H. Y. Yuan, Y. Cao, A. Kamra, R. A. Duine, and P. Yan, Quantum magnonics: when magnon spintronics meets quantum information science, *Phys. Rep.* **965**, 1 (2022).
- [24] D. Lachance-Quirion, Y. Tabuchi, A. Gloppe, K. Usami, and Y. Nakamura, Hybrid quantum systems based on magnonics, *Appl. Phys. Express* **12**, 070101 (2019).
- [25] S. Zheng, Z. Wang, Y. Wang, F. Sun, Q. He, P. Yan, and H. Y. Yuan, Tutorial: Nonlinear magnonics, arXiv:2303.16313.
- [26] T. Neuman, D. S. Wang, and P. Narang, Nanomagnonic Cavities for Strong Spin-Magnon Coupling and Magnon-Mediated Spin-Spin Interactions, *Phys. Rev. Lett.* **125**, 247702 (2020).
- [27] D. S. Wang, T. Neuman, and P. Narang, Spin Emitters beyond the Point Dipole Approximation in Nanomagnonic Cavities, *J. Phys. Chem. C* **125**, 6222 (2021).
- [28] D. S. Wang, M. Haas, and P. Narang, Quantum Interfaces to the Nanoscale, *ACS Nano* **15**, 7879 (2021).
- [29] L. Trifunovic, F. L. Pedrocchi, and D. Loss, Long-Distance Entanglement of Spin Qubits via Ferromagnet, *Phys. Rev. X* **3**, 041023 (2013).
- [30] M. Fukami, D. R. Candido, D. D. Awschalom, and M. E. Flatté, Opportunities for Long-Range Magnon-Mediated Entanglement of Spin Qubits via On- and Off-Resonant Coupling, *PRX Quantum* **2**, 040314 (2021).
- [31] I. C. Skogvoll, J. Lidal, J. Danon, and A. Kamra, Tunable anisotropic quantum Rabi model via magnon—spin-qubit ensemble, *Phys. Rev. Applied* **16**, 064008 (2021).
- [32] W. Xiong, M. Tian, G. Q. Zhang, and J. Q. You, Strong long-range spin-spin coupling via a Kerr magnon interface, *Physical Review B* **105**, 245310 (2022).
- [33] X. L. Hei, X. L. Dong, J. Q. Chen, C. P. Shen, Y. F. Qiao, and P. B. Li, Enhancing spin-photon coupling with a micromagnet, *Phys. Rev. A* **103**, 043706 (2021).
- [34] G. Q. Zhang, Y. P. Wang, and J. Q. You, Theory of the magnon Kerr effect in cavity magnonics, *Sci. China-Phys. Mech. Astron.* **62**, 987511 (2019).
- [35] Y. P. Wang, G. Q. Zhang, D. Zhang, X. Q. Luo, W. Xiong, S. P. Wang, T. F. Li, C. M. Hu, and J. Q. You, Magnon Kerr effect in a strongly coupled cavity-magnon

- system, *Phys. Rev. B* **94**, 224410 (2016).
- [36] Y. P. Wang, G. Q. Zhang, D. Zhang, T. F. Li, C. M. Hu, and J. Q. You, Bistability of Cavity Magnon-Polaritons, *Phys. Rev. Lett.* **120**, 057202 (2018).
- [37] J. M. P. Nair, Z. Zhang, M. O. Scully, and G. S. Agarwal, Nonlinear spin currents, *Phys. Rev. B* **102**, 104415 (2020).
- [38] R. C. Shen, J. Li, Z. Y. Fan, Y. P. Wang, and J. Q. You, Mechanical Bistability in Kerr-modified Cavity Magnomechanics, *Phys. Rev. Lett.* **129**, 123601 (2022).
- [39] R. C. Shen, Y. P. Wang, J. Li, S. Y. Zhu, G. S. Agarwal, and J. Q. You, Long-Time Memory and Ternary Logic Gate Using a Multistable Cavity Magnonic System, *Phys. Rev. Lett.* **127**, 183202 (2021).
- [40] C. Kong, H. Xiong, and Y. Wu, Magnon-Induced Nonreciprocity Based on the Magnon Kerr Effect, *Phys. Rev. Appl.* **12**, 034001 (2019).
- [41] G. Q. Zhang, Y. Wang, and W. Xiong, Detection sensitivity enhancement of magnon Kerr nonlinearity in cavity magnonics induced by coherent perfect absorption, *Phys. Rev. B* **107**, 064417 (2023).
- [42] Z. Zhang, M. O. Scully, and G. S. Agarwal, Quantum entanglement between two magnon modes via Kerr nonlinearity driven far from equilibrium, *Phys. Rev. Research* **1**, 023021 (2019).
- [43] G. Q. Zhang, Z. Chen, W. Xiong, C. H. Lam, and J. Q. You, Parity-symmetry-breaking quantum phase transition in a cavity magnonic system driven by a parametric field, *Phys. Rev. B* **104**, 064423 (2021).
- [44] G. Liu, W. Xiong, and Z. J. Ying, Switchable Superradiant Phase Transition with Kerr Magnons, arXiv:2302.07163.
- [45] H. Siampour, S. Kumar, and S. I. Bozhevolnyi, Chip-integrated plasmonic cavity-enhanced single nitrogen-vacancy center emission, *Nanoscale* **9**, 17902 (2007).
- [46] D. Zhang, X. M. Wang, T. F. Li, X. Q. Luo, W. Wu, F. Nori, and J. Q. You, Cavity quantum electrodynamics with ferromagnetic magnons in a small yttrium-iron-garnet sphere, *npj Quantum Inf.* **1**, 15014 (2015).
- [47] Y. Tabuchi, S. Ishino, A. Noguchi, T. Ishikawa, R. Yamazaki, K. Usami, and Y. Nakamura, *Science*, **349**, 405 (2015).
- [48] X. Zhang, C. L. Zou, L. Jiang, and H. X. Tang, Strongly Coupled Magnons and Cavity Microwave Photons, *Phys. Rev. Lett.* **113**, 156401 (2014).
- [49] M. Goryachev, W. G. Farr, D. L. Creedon, Y. Fan, M. Kostylev, and M. E. Tobar, High-Cooperativity Cavity QED with Magnons at Microwave Frequencies, *Phys. Rev. Applied* **2**, 054002 (2014).
- [50] C. Gonzalez-Ballester, J. Gieseler, and O. Romero-Isart, Quantum Acoustomechanics with a Micromagnet, *Phys. Rev. Lett.* **124**, 093602 (2020).
- [51] T. Niemczyk, F. Deppe, M. Mariani, E. P. Menzel, E. Hoffmann, G. Wild, L. Eggenstein, A. Marx, and R. Gross, Fabrication technology of and symmetry breaking in superconducting quantum circuits, *Supercond. Sci. Technol.* **22**, 034009 (2009).
- [52] D. Vitali, S. Gigan, A. Ferreira, H. R. Böhm, P. Tombesi, A. Guerreiro, V. Vedral, A. Zeilinger, and M. Aspelmeyer, Optomechanical Entanglement between a Movable Mirror and a Cavity Field, *Phys. Rev. Lett.* **98**, 030405 (2007).
- [53] A. Angerer, S. Putz, D. O. Krimer, T. Astner, M. Zens, R. Glattauer, K. Streltsov, W. J. Munro, K. Nemoto, S. Rotter, J. Schmiedmayer, and J. Majer, Ultralong relaxation times in bistable hybrid quantum systems, *Sci. Adv.* **3**, e1701626 (2017).
- [54] J. R. Johansson, P. D. Nation, and F. Nori, Qutip: An open-source Python framework for the dynamics of open quantum systems, *Comput. Phys. Commun.* **183**, 1760 (2012).
- [55] J. R. Johansson, P. D. Nation, and F. Nori, Qutip2: A Python framework for the dynamics of open quantum systems, *Comput. Phys. Commun.* **184**, 1234 (2013).
- [56] H. Fröhlich, Theory of the Superconducting State. I. The Ground State at the Absolute Zero of Temperature, *Phys. Rev.* **79**, 845 (1950).
- [57] S. Nakajima, Perturbation theory in statistical mechanics, *Adv. Phys.* **4**, 363 (1953).
- [58] B. Li, P. B. Li, Y. Zhou, J. Liu, H. R. Li, and F. L. Li, Interfacing a Topological Qubit with a Spin Qubit in a Hybrid Quantum System, *Phys. Rev. Appl.* **11**, 044026 (2019).